Pis'ma v ZhETF, vol. 88, iss. 2, pp. 142 – 146

On superconducting and magnetic properties of iron-oxypnictides

V. Barzykin, L. P. Gor'kov[*+1)]

Department of Physics and Astronomy, University of Tennessee, Knoxville, TN 37996 USA

[*] *National High Magnetic Field Laboratory, Florida State University, Tallahassee, Florida 32310 USA*

[+] *L.D. Landau Institute for Theoretical Physics RAS, 142432 Chernogolovka, Russia*

Submitted 16 June 2008

Pairing symmetry in oxypnictides, a new family of multiband high-T_c superconductors, is partially imposed by the positions of multiple Fermi pockets, which itself can give rise to new order parameters, such as $s_{+,-}$-states or the state of $d_{x^2-y^2}$ symmetry. Other pairing states may appear on small pockets for long range interactions, but they are expected to be sensitive to defects. We identify the competing antiferromagnetic order with the triplet exciton transition in the semi-metallic background and discuss whether its coexistence with superconductivity explains the doping dependence of T_c.

PACS: 74.70.–b, 74.20.–z, 74.20.Rp

Recently discovered superconductors (SC) among the series of iron-oxypnictides[1] with unexpectedly high SC transition temperatures (T_c) reveal a tantalizing resemblance to the cuprates: the layered tetragonal structure, an antiferromagnetic (AFM) order in the normal state and an insulating or semi-metallic behavior for the parent stoichiometric materials with sharp increase in metallicity and the value of T_c for both electron- and hole-doped materials[2].

While the experimental progress is still hindered by the shortage of single crystals, impatience to sort out the physics that governs the puzzling magnetic and electronic behavior in these new superconductors generated an avalanche of theoretical attempts to analyze the new materials from different perspectives, although, most often, using numerical methods. Currently the discussion of physical mechanisms is difficult, in part, because quantitative results often contradict each other. Below we address the phenomena in oxypnictides in a more phenomenological manner, using, at the same time, a number of qualitative features that emerged from previous analyses and of which a consensus was achieved.

We consider possible symmetries of SC order parameters in terms of the SC symmetry classes [3]. The realization of symmetries in a multiband model for oxypnictides leads to interesting implications that depend on the interactions details. We argue that the spin density wave (SDW) in these materials is the triplet excitonic state known for low carrier systems since the 60-s [4, 5] (see Ref.[6] for review). We discuss the coexistence of SDW and SC and the dependence of T_c on doping.

[1)] e-mail: gorkov@magnet.fsu.edu

The reasons why T_c strongly varies among REOFeAs (RE stands for rare earth) [1, 7 – 9], from a few K in the stoichiometric LaOFeAs up to 55 K for RE=Sm[10], remain poorly understood. For instance, T_c is not sensitive to the choise of RE in the cuprates. It was suggested empirically [11] that T_c increases with decreased ionic radii of the rare earth due to the inner chemical pressure. Band structure calculations [12], however, found no dependence on the RE-element. Therefore, we mainly discuss below the doping dependence of T_c.

There is also no consensus about the applicability of the Fermi liquid concepts to oxypnictides. The importance of strong correlations was emphasized in Ref.[13]. To account for the experimental magnetic phase diagram of the parent compound, LaOFeAs [14, 15], localized moments on the d-orbital Fe-ions were postulated in Refs. [16 – 18]. Meanwhile, band structure calculations [12, 19, 20] predict up to five small 2D Fermi surface (FS) sheets in LaOFeAs; the material would then constitute a low carrier 2D ionic metal that, within the limits of accuracy of the method, shows a proximity to either ferro- or AFM-instabilities. According to Ref.[21], LaOFeAs must be itinerant. The tendency to AFM state ascribed to "nesting" between different FS sheets.

The metallic behavior [1, 22] above T_c and the very onset of SC present a direct proof of an itinerant character for the carriers in the oxypnictides. Therefore, FS sheets *must* exist, at least at finite doping (see, e.g., Ref.[20]). In Ref.[19] these FS, as it was mentioned above, were obtained from the Density Functional calculations. Note that all numerical methods become especially vulnerable near the chemical potential, E_F, and often lead to conflicting results for the density of states

(DOS), such as asymmetries in DOS at E_F that would contradict observations of SC for both electron [1] and hole [2] doping [23].

We accept below the model for the electronic structure of the oxypnictides with the FS topology that practically coincides with the one in Ref.[19, 21], except that we omit the small 3D hole pocket at the Z-point in the large Brillouin Zone (BZ) (1Fe/cell). In Figure there are

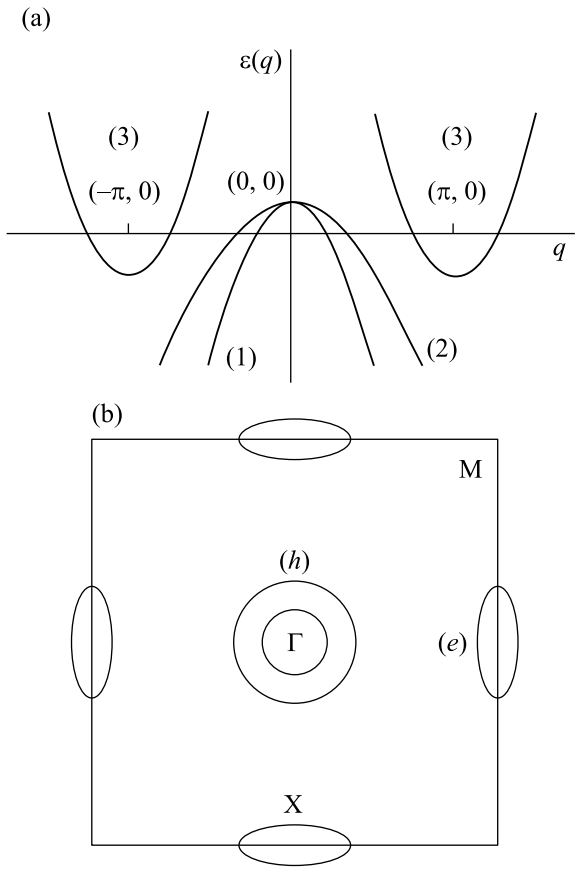

Schematic electronic spectrum (a) and Fermi surfaces (b) of LaOFeAs in the unfolded Brillouin zone. Two different hole Fermi surfaces form around the Γ point, while the electron pockets appear at the X-points

two hole pockets in the center of the BZ that appear as a result of the degeneracy of the spectrum at the Γ-point [12, 20]. Two electron pockets on the sides of the square, $(0, \pi)$ and $(\pi, 0)$, have a two-fold anisotropy.

Such FS structure corresponds, at the stoichiometric composition, to the compensated semi-metal, with equal volumes occupied by electrons and holes. Electron doping would diminish sizes of the hole-pockets, and vice versa. Judging from experiments [1, 2], DOS on both sides of the Fermi level, $\nu(E_F)$, is approximately the same and *stays constant* in its vicinity, reflecting the two-dimensionality of FS. This is not the case in band structure calculations [12, 13, 19]. On the other hand, if DOS *were a constant, the transition temperature, T_c, could not vary with concentration* in the BCS-like fashion:

$$T_c(x) \propto \exp(-1/V\nu(x, E_F)). \qquad (1)$$

It is known experimentally that SC competes with AFM: no magnetic order has been observed either in the normal or SC state for $La(O_{1-x}F_x)FeAs$ ($T_c = 26\,K$) [24]. However, if the SDW and SC orders did coexist, this could provide a natural mechanism for a variable DOS near E_F[22].

For what follows it is helpful to consider the characteristic energy scales of oxypnictides. These are as follows: the Debye temperature is $\omega_D = 282\,K$ [22]; the energies above and below E_F spanned by the iron d-orbitals are in the range $\Delta E \sim 2\,eV$, while the electron- and hole-pockets' depths are of the order of $0.1 - 0.2\,eV \sim 2000\,K \ll \Delta E$ [12, 19, 20]; the temperature of the SDW singularity in the parent compound LaOFeAs is $T_{SDW} \sim 150\,K$ [14], and the corresponding DOS energy gap, as seen in the infrared reflectance [22] is small: $\sim 150{-}350\,cm^{-1}$. With T_c ranging from $\sim 4\,K$ to $55\,K$, it seems possible to analyze the properties of oxypnictides at the mean field level.

We start with the symmetry analysis for the SC order parameters on multiple FS's in Figure in the absence of SDW. Some results are also rigorously applicable when the SDW and either the hole- or electron-pockets are fully eliminated by the proper doping. Note that the pockets' areas in Figure are rather small (of order 10% or less of BZ, e.g.,see Ref.[19]). Let $\Delta_i(\mathbf{p})$ be the SC parameter on the i^{th} FS. The self-consistency relation that defines $\Delta_i(\mathbf{p})$ through the anomalous Gor'kov functions, $F_i(\omega_n, \mathbf{p})$, is of the form:

$$\Delta_i(\mathbf{p}) = T \sum_{j;\omega_n} \int V^{i,j}(\mathbf{p} - \mathbf{p}') d\mathbf{p}' F_j(\omega_n, \mathbf{p}'), \qquad (2)$$

where $V^{i,j}(\mathbf{p}-\mathbf{p}')$ is the Fourier component of the interaction. If the pockets are small, the momentum transfer, $\mathbf{p} - \mathbf{p}'$, inside each pocket is small as well, so that one can replace $V^{i,j}(\mathbf{p} - \mathbf{p}')$ with $V^{i,j}(0)$, if, as we discuss below, the interaction is short range. This, of course, favors momentum independent gaps and, hence, a singlet pairing.

The interaction Hamiltonian for four separate Fermi surfaces can be written in the BCS-like form (compare, for example, with Ref. [25]):

$$H_{\rm int} = \frac{1}{2} \sum_{\mathbf{p},\mathbf{p}'} \sum_{ij\sigma\sigma'} \tilde{V}^{i,j}_{\mathbf{p},\mathbf{p}'} a^\dagger_{i\sigma\mathbf{p}} a^\dagger_{i\sigma'-\mathbf{p}} a_{j\sigma'\mathbf{p}'} a_{j\sigma-\mathbf{p}'}, \qquad (3)$$

and

$$\tilde{V}^{i,j}_{\mathbf{p},\mathbf{p}'} = V^{i,j}(\mathbf{p}-\mathbf{p}')w_i^*(\mathbf{p})w_i^*(-\mathbf{p})w_j(\mathbf{p}')w_j(-\mathbf{p}'), \quad (4)$$

where $w_i(\mathbf{p})$ are the periodic Bloch functions. The anomalous Gor'kov functions F, $F^\dagger$ are defined in the real space. Correspondingly, the wave functions of the Cooper pair are proportional to $\langle\Psi_i(\mathbf{r})\Psi_j(\mathbf{r}')\rangle$, where $\Psi_i(\mathbf{r})$ is the full field operator. Therefore, $\Delta_i(\mathbf{p})$ differ from just the averages $\langle a_{i,\mathbf{p}}a_{i,-\mathbf{p}}\rangle$, where $\mathbf{p}$ is now the quasi-momentum, by the factors $w_i(\mathbf{p})$ and $w_i(-\mathbf{p})$. The derivation of the Bloch functions and of the energy spectrum near the double-degenerate Γ-point will be given elsewhere.

To apply the approach of Ref.[3] to the multiband model in Figure, it is necessary to account for the fact that the transformations of the point group D_4 may interchange the electronic FSes. After linearization in Δ_i, Eq.(2) determines the transition temperature for each irreducible representation. To enumerate all possible symmetries, we apply the transformations of the D_4 group to the column of $\{\Delta_{h1}, \Delta_{h2}, \Delta_{eX}, \Delta_{eY}\}$. After calculating characters we find three identical representations and the one belonging to the non-trivial class, B_2. The latter constitutes the $d_{x^2-y^2}$ state which, if one neglects the momentum dependence of $V^{i,j}(\mathbf{p}-\mathbf{p}')$, signifies a gapless state on the hole pockets in Figure. (For momentum dependent interactions, however, the hole pockets become weakly gapped with zeroes along the diagonals in Figure.) Recent high resolution PES experiments[26] have indeed detected gapless hole FSes at the Γ-point.

To account for all the features of the band structure in Figure, we perform this analysis in a more explicit manner. The interaction between the electrons forming a Cooper pair on Fermi pockets shown in Figure takes the following form:

$$V = \begin{pmatrix} u & u & t & t \\ u & u & t & t \\ t & t & \lambda & \mu \\ t & t & \mu & \lambda \end{pmatrix}. \quad (5)$$

Here $\lambda = V^{eX,eX} = V^{eY,eY}$ is the interaction on the same electron pocket at the X-point, $\mu = V^{eX,eY}$ couples electron pockets at $(\pi,0)$ and $(0,\pi)$, $u = V^{h1,h1} = V^{h2,h2} = V^{h1,h2}$ characterizes the BCS interactions for electrons on two different hole Fermi surfaces at the Γ-point, while $t = V^{h,eX} = V^{h,eY}$ is the coupling that connects the Cooper pairs at the X-points and the Γ-point. The form of the interaction matrix V for the two hole pockets at the Γ-point follows from the degeneracy of the bands at the Γ-point.

Solution of the linearized gap equation,

$$\Delta_i = \sum_j \bar{V}^{i,j}\Delta_j \ln\frac{2\gamma\bar{\omega}}{\pi T_c}, \quad (6)$$

where $\bar{\omega}$ is the cut-off in the Cooper logarithm and

$$\bar{V}^{i,j} \equiv -\frac{1}{2}V^{i,j}\nu_j, \quad (7)$$

determine the T_c values for the order parameters of different symmetries. Introducing effective coupling g,

$$T_c = \frac{2\gamma\bar{\omega}}{\pi}e^{-2/g}, \quad (8)$$

we find three different solutions:

1) For the non-trivial, $d_{x^2-y^2}$ symmetry – the energy gap on different X-pockets changes sign:

$$\Delta_1 = \Delta_2 = 0, \quad \Delta_3 = -\Delta_4 = \Delta, \quad (9)$$

$$g = (\mu-\lambda)\nu_3. \quad (10)$$

2) The two solutions that can belong to the so-called s_+, s_- states, where the energy gap at the X-points have the same sign, while at the Γ-point it may have a different sign, with

$$2g_{+,-} = -u(\nu_1+\nu_2) - (\lambda+\mu)\nu_3 \pm \pm\sqrt{(u(\nu_1+\nu_2)-(\lambda+\mu)\nu_3)^2 + 8t^2\nu_3(\nu_1+\nu_2)} \quad (11)$$

and

$$\Delta_1 = \frac{\nu_1\Delta_2}{\nu_2} = \kappa\Delta, \quad \Delta_3 = \Delta_4 = \Delta, \quad (12)$$

where $\kappa^{-1} = -(g_{+,-} + u(\nu_1+\nu_2))/(t\nu_1)$.

In Ref. [21] it was assumed that the strongest interactions may be due to the SDW channel. In our notations it would mean large V^{e-h} matrix elements in Eqs.(3),(5), (6). The "$s^{+(-)}$" superconductivity [21] for gaps on the electron and hole FS indeed follows from Eqs.(11), (12) in this limit. (Such a state does not follow from the symmetry arguments).

We turn now to the changes in Figure introduced by the presence of SDW. The AFM phase itself can be described in terms of the local iron moments provided the exchange integrals are such that the (nn) exchange parameter, J_1, is smaller than the (nnn) integral, J_2. This relation leads to the AFM state with the correct structure vector $\mathbf{Q} = (0,\pi)$ or $(\pi,0)$ [16–18]. For J_1, J_2 experiments would then give an estimate $J \sim 150-250\,\mathrm{K}$ [18, 14]. (Theoretical estimates vary strongly from $\sim 0.5\,\mathrm{eV}$ [16] to $\sim 50-100\,\mathrm{K}$[13]).

Exchange integrals in the Hamiltonian for local spins determine the Neèl temperature, T_N. However, in this case AFM introduces no new scale in the momentum space: the magnon spectrum extends over the whole BZ. Therefore, the same arguments as above apply to contributions into the $e-e$ interactions that originate from the degrees of freedom of local spins : if FS pockets are of small size, the dependence on momentum transfer in the scattering matrix element of two electrons inside the same pocket may be omitted.

SDW in oxypnictides is commonly attributed to the strong nesting in the literature, i.e., the congruency in the FS shapes between electron and hole pockets in Figure (see e.g. in Refs. [15, 19, 21, 27]). The generalized magnetic susceptibility, $\chi(\mathbf{q})$, numerically calculated in Refs.[19, 21], demonstrates indeed the strongly peaked character at $\mathbf{Q} = (0, \pi)$. Among advantages of this scenario, in the first place, is that it leads naturally to the observed AFM structure vector[14]. Note, however, that the vector $\mathbf{q} = \mathbf{Q}$, in our opinion, does not justify the nesting scenario. Indeed, the electron pocket contains only half of the carriers' number at the Γ – point (for the parent compound), and, in addition, is anisotropic. Therefore, we suggest that the numerical results [19, 21] do not distinguish between the nesting scenario and the formation of the exciton phase [4–6], which comes about, first of all, due to the Coulomb interactions between the electron and the hole bands. (In the main approximation the instability is degenerate with respect to formation of singlet or triplet excitons [6].)

For the AFM superstructure with vector $\mathbf{Q} = (0, \pi)$, the two hole-like bands and one electron band in Figure overlap, leading to a partially gapped spectrum because of non-congruency of pockets. The second electron pocket remains untouched. Assuming the interactions discussed above, it is natural to expect smaller T_c due to partially gapped spectra. As SDW is gradually lifted with doping, the T_c-value is expected to increase. This process, at first glance, could provide a mechanism for the variation of T_c at low doping.

No rigorous theoretical results are available for the excitonic transition beyond the Hartree-Fock approximation (see, e.g., in Ref.[6]). Qualitatively, dependence of such a phase on doping is as follows. The value of T_N or, better, the gap [22] provides an estimate of the energy gain at the phase formation. SDW would be destroyed when the change in the energy due to carriers poured into the electron or hole pockets, becomes of the same order. Rough estimates for the carriers' concentration give realistic values for x a few percent (the estimate is sensitive to the numerical results for the effective mass that vary considerably [12, 19, 23]).

In LaOFeAs the SDW-anomaly disappears already at 3% F-doping, while T_c continues to increase with doping up to 28 K at $6 \sim 8$ % F-content [22]. The AFM feature seen at 150K in pure NdOFeAs [28] rapidly disappears at the oxygen doping [29] below the T_c-maximum (a sudden increase in T_c [29] can be a hallmark of a change in the ground state). One, hence, concludes that SDW and SC change differently and independently with doping and the SDW is destroyed faster.

The above brings us back to the problem that in the BCS-like Eq.(1) for T_c the two-dimensional DOS does not vary with the carriers' concentration and the concentration dependence of T_c, hence, is to reflect new mechanisms. It is possible that doping concentrations up to 15% are not so small and, in view of the ionic character of the coupling between oppositely charged layers, produces strong effects on the lattice [11, 29]. Another, although a more exotic, interpretation in frameworks of rigid bands, could signify an enhancement in the interactions strength. No changes in the phonon spectrum have been reported [22]. The Coulomb screening in 2D in the Thomas-Fermi limit does not depend on carriers concentrations either. (Actual Coulomb screening acquires three-dimensional character through charges in the adjacent planes). As to AFM fluctuations (e.g., in [21]), in view of the above, one may expect that AFM fluctuations are already significantly suppressed in this doping range.

The low sensitivity of T_c to defects favors the gapped SC order. (The classes that allow nodes along a FS, of course, should be same as in Ref.[3] and have been recently discussed anew, e.g., in Refs.[30, 31]). The observation of gapless FS at the Γ-point [26] points unambiguously in favor of the $d_{x^2-y^2}$ SC order for the electronically doped materials. In other words, at high enough doping level SC pairing is not electron-hole symmetric. For the d-wave pairing in Eq.(10) we can assume negative λ (phonons) and positive μ (Coulomb repulsion).

In summary, we have enumerated possible symmetries of SC order for the FS topology now broadly accepted for the oxypnictides in the literature. Small sizes of FS in the frameworks of a semi-metallic picture allowed to narrow significantly the number of SC states. Among the three SC states there exists the symmetry class analogous to the popular $d_{x^2-y^2}$ pairing in the cuprates. Its realization in oxypnictides predicts the whole ungapped internal (hole) pockets, in excellent agreement with the recent high resolution PES experiments [26]. We identified onset of the AFM order in the parent materials with transition into the triplet exciton state caused by Coulomb interaction in this family of semi-metallic compounds. While at low doping AFM

affects the band energy spectrum and the resulting variation in DOS can explain the dependence of T_c on concentration, experimentally T_c continues to increase even after AFM is destroyed. Our results show that SC for electron and hole doping have a different symmetry. We have also discussed possible mechanisms for the increase of T_c with doping.

The authors are thankful to Z. Fisk, M. Sadovskii, and G.Teite'lbaum for helpful discussions. This work was supported by NHFML through the NSF Cooperative agreement No. DMR-008473 and the State of Florida.

1. Y. Kamihara, T. Watanabe, M. Hirano, and H. Hosono, J. Am. Chem.Soc. **130**, 3269 (2008).
2. H.-H. Wen, G. Mu, L. Fang et al., Europhys. Lett. **82**, 17009 (2008).
3. G. E. Volovik and L. P. Gor'kov, Pis'ma v Zh. Eksp. Teor. Fiz. **39**, 550 (1984) [JETP Lett. **39**, 674 (1984)]; Zh. Eksp. Teor. Fiz. **88**, 1412 (1985) [JETP **61**, 843 (1985)].
4. N. F. Mott, Phil. Mag. **6**, 287 (1961).
5. R. S. Knox, Solid State Phys. Suppl. **5**, 100 (1963).
6. B. I. Halperin and T. M. Rice, in: F. Seitz, D. Turnball, and H. Ehrenfest, Eds., Solid State Physics, v. **21**, Academic Press, N.Y., 1968, p. 155.
7. X. H. Chen, T. Wu, G. Wu et al., arXiv:0803.3603 (2008).
8. G. F. Chen, Z. Li, D. Wu et al., arXiv:0803.3790 (2008).
9. Z.-A. Ren, J. Yang, W. Lu et al., arXiv:0803.4283 (2008).
10. Z.-A. Ren, W. Lu, J. Yang et al., arXiv:0804.2053 (2008); Chin. Phys. Lett. **25**, 2215 (2008).
11. W. Lu, X.-L. Shen, J. Yang et al., arXiv:0804.3725 (2008).
12. I. A. Nekrasov, Z. V. Pchelkina, and M. V. Sadovskii, JETP Lett. **87**, 647 (2008).
13. K. Haule, J. Y. Shim, and G. Kotliar, arXiv: 0803.1279 (2008); K. Haule and G. Kotliar, arXiv:0805.0722 (2008).
14. C. de la Cruz, Q. Huang, J. W. Lynn et al., arXiv:0804.0795 (2008).
15. M. A. McGuire, A. D. Christianson, A. S. Sefat et al., arXiv:0804.0796 (2008).
16. Q. Si and E. Abrahams, arXiv:0804.2480 (2008).
17. T. Yildirim, arXiv:0804.2252 (2008).
18. C. Fang, H. Yao, W.-F. Tsai et al., arXiv:0804.3843 (2008).
19. D. J. Singh and M.-H. Du, arXiv:0803.0429 (2008).
20. K. Kuroki, S. Onari, R. Arita et al., arXiv: 0803.3325 (2008).
21. I. I. Mazin, D. J. Singh, M. D. Johannes, and M. H. Du, arXiv:0803.2740 (2008).
22. J. Dong, H. J. Zhang, G. Xu et al., arXiv:0804.3426 (2008).
23. Z. P. Yin, S. Lebègue, M. J. Han et al., arXiv: 0804. 3355 (2008).
24. Y. Qiu, M. Kofu, W. Bao et al., arXiv: 0805.1062 (2008).
25. D. F. Agterberg, V. Barzykin, and L. P. Gor'kov, Phys. Rev. B **60**, 14868 (1999).
26. X. Jia, H. Liu, W. Zhang et al., arXiv: 0806.0291 (2008).
27. S. Raghu, X.-L. Qi, C.-X. Liu et al., arXiv: 0804.1113 (2008).
28. G. F. Chen, Z. Li, D. Wu et al., arXiv:0803.4384 (2008).
29. Z.-A. Ren, G.-C. Che, X.-L. Dong et al., arXiv:0804.2582 (2008).
30. Z.-H. Wang, H. Tang, Z. Fang, and X. Dai, arXiv 0805.0736 (2008).
31. Y. Wan and Q.-H. Wang, arXiv: 0805.0923 (2008).